12th International Symposium on Turbulence and Shear Flow Phenomena (TSFP12)
Osaka, Japan (Online), July 19-22, 2022

INVARIANT MOMENT AND PDF SOLUTIONS OF WALL-BOUNDED TURBULENT SHEAR FLOWS

Dominik Plümacher
Department of Mechanical Engineering
Technical University of Darmstadt
Otto-Bernd-Str. 2, 64287 Darmstadt, Germany
pluemacher@fdy.tu-darmstadt.de

Martin Oberlack
Department of Mechanical Engineering
Technical University of Darmstadt
Otto-Bernd-Str. 2, 64287 Darmstadt, Germany
oberlack@fdy.tu-darmstadt.de

Sergio Hoyas
Instituto Universitario de Matemática Pura y Aplicada, UP València,
Camino de Vera, 46024 València, Spain
serhocal@mot.upv.es

ABSTRACT

In a recent publication Oberlack *et al.* (2022) by the last two authors, they showed that velocity moments of arbitrary order can be derived as invariant solutions of the multi-point moment equations by means of the symmetry-based turbulence theory. They applied it to the log-region as well as to the deficit region in the centre of a channel flow. The results were validated with a new channel flow DNS at $Re_\tau = 10^4$ with high accuracy and up to moment order 6. Presently we have significantly extended it by computing a invariant solutions for the probability density function (PDF), which is formally the next higher-level statistical description of turbulence. This new solution is believed to be the first exact solution to Lundgren's PDF equation, and in the sequel we show that the above moments can be generated from it.

INTRODUCTION

To treat the complex flow behaviour of turbulent fluids mathematically, a statistical approach has been the most successful so far. For a complete mathematical description, however, an infinite number of coupled equations is usually required, a fact that was already known to Reynolds. For practical applications it is therefore necessary to reduce this set of equations to a finite set by some form of closure procedure, This, however, considerably limits the prediction accuracy of such an approach. Quite early on, it was observed that for canonical flows, certain distinguished regions can be identified in which a universal behaviour is exhibited and corresponding simplified equations can be derived heuristically. Nowadays, these results are usually subsumed under the term *scaling law* and are essentially based on similarity arguments, which in turn often exploit, at least indirectly underlying symmetries of the physical process. Probably one of the first examples of such a result is the well-known logarithmic law of the wall due to von Kármán (1930). A downside of von Kármán's reasoning, however, is that it is not based on the Navier-Stokes equations, and therefore are not derived from "first principles" in this sense. This aspect was not remedied in the following decades of research in modified versions of the log-law, see e.g. Barenblatt (1993). One of the first works that derived a scaling law as a self-similar solution is the work of von Kármán & Howarth (1938) on the decay of isotropic turbulence. Subsequently, this approach was applied very successfully to a large number of flows.

The idea of applying the methods of symmetry theory for a systematic derivation of "scaling laws" via self-similar solutions was probably first proposed by Oberlack (2001). Further work followed even for more complex flows with rotation, wall transpiration, and many more, see Avsarkisov *et al.* (2014); Oberlack *et al.* (2015); Sadeghi *et al.* (2018). However, all these approaches were limited to low order moments. For all these scaling laws statistical symmetries played an essential role. These were first observed by Oberlack & Rosteck (2010) in the infinite sequence of the multipoint moment equations (MPME). Furthermore, it was shown by Wacławczyk *et al.* (2014) that these symmetries are related to the phenomena of intermittency and of non-Gaussian behaviour in turbulence - both of which illustrate well-known, central characteristics of turbulent flows and which, with the latter, offer a unique quantification in terms of symmetries. The infinite sequence of the multipoint moment equations is formed from the Navier-Stokes equations,

$$\frac{\partial U_i}{\partial t} + U_k \frac{\partial U_i}{\partial x_k} + \frac{\partial P}{\partial x_i} - \nu \frac{\partial^2 U_i}{\partial x_k \partial x_k} = 0 \qquad i = 1,2,3 \tag{1}$$

$$\frac{\partial U_i}{\partial x_i} = 0 \tag{2}$$

where $t \in \mathbb{R}^+$, $\boldsymbol{x} \in \mathbb{R}^3$, $\boldsymbol{U} = \boldsymbol{U}(\boldsymbol{x},t)$, $P = P(\boldsymbol{x},t)$ and ν respectively represent time, position vector, instantaneous velocity vector, pressure, and kinematic viscosity. When dealing with statistical properties, typically, Reynolds's decomposition is used, i.e., $U_k = \overline{U}_k + u_k$, where $\overline{(\,.\,)}$ denotes averaging and u_k is the turbulent fluctuation. We depart here from the usual approach to analyse moment equations based on the fluctuations and use instead statistical moments that are composed of the full instantaneous velocities. The main ideas and steps of this approach are briefly illustrated in the following section.

HIGH-ORDER MOMENT SCALING LAWS

For the subsequent new findings on the PDF, the central results for the high velocity moments in turbulent shear flows close to the wall will be outlined first.

The essential ingredients for the construction of invariant solutions are so-called symmetry transformations which refer to a variable transformation

$$\boldsymbol{x}^* = \boldsymbol{\phi}(\boldsymbol{x},\boldsymbol{y};a), \qquad \boldsymbol{y}^* = \boldsymbol{\psi}(\boldsymbol{x},\boldsymbol{y};a) \tag{3}$$

which leaves a differential equation form invariant when it is written in the new $*$-variables, i.e. if the following holds

$$\begin{aligned} &\boldsymbol{F}\left(\boldsymbol{x},\boldsymbol{y},\boldsymbol{y}^{(1)},\boldsymbol{y}^{(2)},\dots,\boldsymbol{y}^{(p)}\right) = 0 \\ \Leftrightarrow \quad &\boldsymbol{F}\left(\boldsymbol{x}^*,\boldsymbol{y}^*,\boldsymbol{y}^{*(1)},\boldsymbol{y}^{*(2)},\dots,\boldsymbol{y}^{*(p)}\right) = 0 \end{aligned} \tag{4}$$

where $\boldsymbol{y}^{(p)}$ denotes the set of all p^{th} derivatives of $\boldsymbol{y}$.

The basis for the analysis in Oberlack *et al.* (2022) are the multi-point moment equations

$$\frac{\partial H_{i_{\{n\}}}}{\partial t} + \sum_{l=1}^{n}\left[\frac{\partial H_{i_{\{n+1\}}[i_{(n)}\mapsto k_{(l)}]}[\boldsymbol{x}_{(n)}\mapsto \boldsymbol{x}_{(l)}]}{\partial x_{k_{(l)}}} + \frac{\partial I_{i_{\{n-1\}}[l]}}{\partial x_{i_{(l)}}} - \nu \frac{\partial^2 H_{i_{\{n\}}}}{\partial x_{k_{(l)}}\partial x_{k_{(l)}}}\right] = 0 \tag{5}$$

with the multi-point velocity moments defined as follows

$$H_{i_{\{n\}}} = H_{i_{(1)}\dots i_{(n)}} = \overline{U_{i_{(1)}}(\boldsymbol{x}_{(1)},t)\cdot\ldots\cdot U_{i_{(n)}}(\boldsymbol{x}_{(n)},t)} \tag{6}$$

and $I_{i_{\{n-1\}}[l]}$ contains the pressure, with details may be taken from Oberlack & Rosteck (2010). In the limit of vanishing viscosity $\nu \to 0$ equation (5) admits the following three-parameter scaling groups

$$\begin{aligned} \bar{T}_{Scale}:\ & x_2^* = \mathrm{e}^{a_{Sx}} x_2,\ \bar{U}_1^* = \mathrm{e}^{a_{Sx}-a_{St}+a_{Ss}}\bar{U}_1, \dots, \\ & \overline{U_1^n}^* = \mathrm{e}^{n(a_{Sx}-a_{St})+a_{Ss}}\overline{U_1^n} \end{aligned} \tag{7}$$

The symmetries associated with a_{Sx} and a_{St} are scaling of time and space that come from the Navier-Stokes equations. The parameter a_{Ss} refers to a scaling symmetry that is purely statistical in nature and only occurs in the statistical equation, which, although infinite dimensional, are linear. This is also in clear contrast to equations that follow from the Reynolds decomposition. These appear non-linear by expressions like the production term. It should be noted, however, that this is ostensibly the case, for the equations formed from the Reynolds decomposition as well as the H-formulation used here as completely equivalent. Even more, in the H-formulation in equation (5) on sees that this forms an infinite set of conversation equations. The scaling referring to a_{Ss} denote a measure of intermittency and the further statistical symmetry

$$\begin{aligned} \bar{T}'_{\{n\}}:\ & t^* = t,\ \boldsymbol{x}^*_{(i)} = \boldsymbol{x}_{(i)}, \\ & \bar{\boldsymbol{U}}^* = \bar{\boldsymbol{U}} + \boldsymbol{a},\ \mathbf{H}^*_{\{n\}} = \mathbf{H}_{\{n\}} + \mathbf{a}^H_{\{n\}} \end{aligned} \tag{8}$$

defines non-gaussianty (Wacławczyk *et al.*, 2014).

For the following comparison with the DNS data, we only consider one-point statistics, i.e. we apply $\boldsymbol{x} = \boldsymbol{x}_{(1)} = \boldsymbol{x}_{(2)} = \ldots = \boldsymbol{x}_{(n)}$ and further limit ourselves to the moments of the stream-wise velocity U_1. Hence the $H_{i_{\{n\}}}$ reduce to one-point moments $\overline{U_1^n}$.

In Oberlack *et al.* (2022) it is rigorously shown, and this shall not be repeated here, how from this for the log region arbitrarily high moment scaling laws are generated. The key parameter for the log-law is the wall shear stress velocity $u_\tau = \sqrt{\tau_w/\rho}$, where τ_w is the wall shear stress and ρ is the density. u_τ uniquely determines the only velocity scale in the problem. u_τ implies that a scaling of the mean velocities according to Eq. (7) with arbitrary a_{Sx}, a_{S_t} and a_{Ss} is no longer feasible. Hence, in terms of symmetry theory, u_τ is symmetry breaking for the mean velocity $\overline{U}_1$ and for the group parameters in Eq. (7) this implies $a_{Sx} - a_{St} + a_{Ss} = 0$ and it follows

$$\bar{U}_1^+ = \frac{1}{\kappa}\ln\left(y^+\right) + B \tag{9}$$

$$\overline{U_1^n}^+ = C_n\left(y^+\right)^{\omega(n-1)} - B_n,\ \text{for } n \geq 2 \tag{10}$$

$$C_n = \alpha \mathrm{e}^{\beta n},\ B_n = \tilde{\alpha}\mathrm{e}^{\tilde{\beta} n},\ \text{for } n \geq 2 \tag{11}$$

with κ and ω are related to the group parameters from (8) and the scaling symmetries (7) as follows $\kappa = a_{Sx}/a_1^H$ and $\omega = 1 - a_{St}/a_{Sx}$. ω is the exponent of the second moment and apparently scales all higher moments.

The following result on the scaling laws in the centre of the channel is also taken from Oberlack *et al.* (2022). Not imposing any symmetry breaking in the first place for the centre of the channel, the so-called deficit region, the following scaling laws were generated

$$\frac{\overline{U_1^n}^{(0)} - \overline{U_1^n}}{u_\tau^n} = C'_n\left(\frac{x_2}{h}\right)^{n(\sigma_2-\sigma_1)+2\sigma_1-\sigma_2} \tag{12}$$

$$\text{with } C'_n = \alpha' \mathrm{e}^{\beta' n} \tag{13}$$

with the scaling exponents of the first and second moments, σ_1 and σ_2, are related to the scaling symmetries (7) as follows $\sigma_1 = 1 - a_{St}/a_{Sx} + a_{Ss}/a_{Sx}$ and $\sigma_2 = 2(1 - a_{St}/a_{Sx}) + a_{Ss}/a_{Sx}$. Further, $\overline{U_1^n}^{(0)}$ is the n-th U_1-moment at the centre line of the channel.

Data clearly show, that $\sigma_1 \simeq \sigma_2 \simeq 1.95$ and hence $2\sigma_1 - \sigma_2 = a_{Ss}/a_{Sx}$ remains in the exponent for all moments, which, as no longer scaling with n, implies strong anomalous scaling. This is fully in line with the fact, that a_{Ss} is a measure of intermittency which is the dominating effect in the channel centre.

Verification of the log-region scaling (9) and (10) is shown in figures 1, while clear evidence of the extended deficit scaling (12) is shown in 2, where both images are reproductions from Oberlack *et al.* (2022).

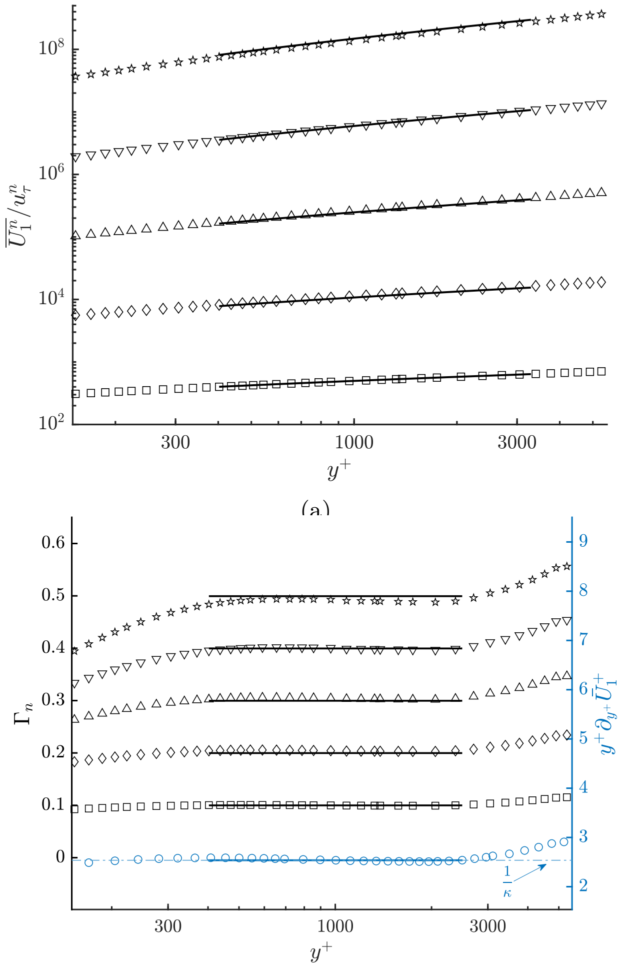

(b)

Figure 1: Symbols from DNS data $n = 1$: ○, $n = 2$: □, $n = 3$: ◇, $n = 4$: △, $n = 5$: ▽, and $n = 6$: ☆; (a): moments $\overline{U_1^n}^+$; ——: Eq. (10) with coefficients fitted to DNS data for $n \geq 2$. (b): Left axis: indicator function $\Gamma_n = \frac{y^+}{\overline{U_1^n}^+ + B_n} \frac{\mathrm{d}\overline{U_1^n}^+}{\mathrm{d}y^+}$ for (10); ——: $\Gamma_n = \omega(n-1)$ with $\omega = 0.10$ and $n \geq 2$. Right axis: log-indicator function $\Gamma = y^+ \partial_{y^+} \bar{U}_1^+ = \kappa^{-1}$ according to (9) with $\kappa = 0.394$. Figures are taken from Oberlack *et al.* (2022)

Although in the derivation of the multi-point moment equations (5) the probability density function (PDF) has been used only formally, information of the PDF has not been incorporated. Thus, the basis of the aforementioned symmetries and resulting scaling laws are implicitly based on the PDF, which will be examined in detail in the following chapter.

PDF BASED SCALING LAWS

A similar construction as outlined in the first section can be done for the probability density functions (PDFs), subsequently written in increment form. Thus,

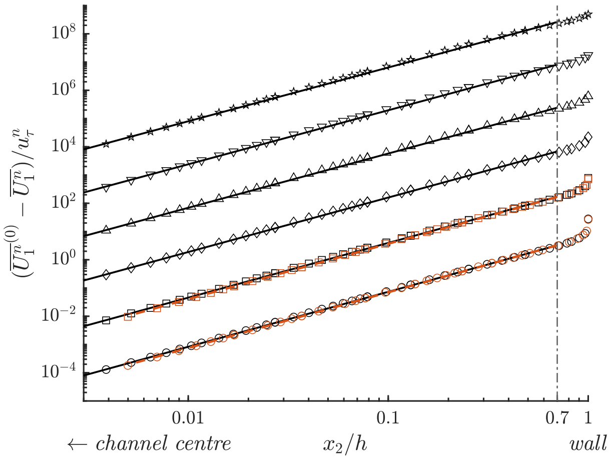

Figure 2: Deficit scaling of $\overline{U_1^n}$ of order $n = 1,\ldots 6$ in the channel centre. Solid lines are according to Eq. (12). Symbols, DNS data as in Fig. 1. Red dashed lines and symbols: $Re_\tau = 5200$ Lee & Moser (2015). Vertical dotdashed line: Limit for the channel's centre region defined by equation (12). Figure is taken from Oberlack *et al.* (2022).

the one- and two-point PDF are defined by

$$
\begin{aligned}
&f_1(\boldsymbol{v};\boldsymbol{x},t) = \langle \delta(\boldsymbol{v} - \boldsymbol{U}(\boldsymbol{x},t)) \rangle, \\
&f_2(\boldsymbol{v},\boldsymbol{w}_{(2)};\boldsymbol{x},\boldsymbol{r}_{(2)},t) = \\
&\langle \delta(\boldsymbol{v} - \boldsymbol{U}(\boldsymbol{x},t))\, \delta(\boldsymbol{w}_{(2)} - \boldsymbol{U}(\boldsymbol{x}+\boldsymbol{r}_{(2)},t) + \boldsymbol{U}(\boldsymbol{x},t)) \rangle \quad (14)
\end{aligned}
$$

were $\boldsymbol{w}_{(j)}$ denotes the sample space variable for the velocity difference between points $\boldsymbol{x} = \boldsymbol{x}_1$ and $\boldsymbol{x} + \boldsymbol{r}_{(j)}, j = 2,3,\ldots$, i.e. $\boldsymbol{U}(\boldsymbol{x}+\boldsymbol{r}_{(j)},t) - \boldsymbol{U}(\boldsymbol{x},t)$, and δ denotes Dirac's delta function. The analogue definition for the n-point PDF f_n is straight-forward.

The associated equations governing the time-evolution of the hierarchy of PDFs $\{f_n : n = 1,2,3\ldots\}$ are the Lundgren-Monin-Novikov (LMN) equations, first derived by Lundgren (1967) and independently by Monin (1967). The first equation for the one-point PDF f_1 reads

$$
\begin{aligned}
\frac{\partial f_1}{\partial t} + \boldsymbol{v}\cdot\nabla_{\boldsymbol{x}} f_1 + \nabla_{\boldsymbol{v}} \cdot \int \nabla_{\boldsymbol{r}_2} G(\boldsymbol{r}_2)\,(\boldsymbol{w}_2 \cdot \nabla_{\boldsymbol{r}_2})^2 f_2 \,\mathrm{d}\boldsymbol{w}_2 \mathrm{d}\boldsymbol{r}_2 \\
+ \nu \nabla_{\boldsymbol{v}} \cdot \int \boldsymbol{w}_2 \Delta_{\boldsymbol{r}_2} f_2 \;\delta(\boldsymbol{r}_2)\,\mathrm{d}\boldsymbol{w}_2 \mathrm{d}\boldsymbol{r}_2 = 0 \quad (15)
\end{aligned}
$$

where $G(\boldsymbol{r}) = (4\pi)^{-1}|\boldsymbol{r}|^{-1}$, and $\nabla_{\boldsymbol{x}}, \nabla_{\boldsymbol{r}_{(j)}}$, etc., denote the nabla operator w.r.t. the variable $\boldsymbol{x}$, $\boldsymbol{r}_{(k)}$, etc.. Similarly, $\Delta_{\boldsymbol{r}_{(j)}}$ denotes the Laplace operator w.r.t. $\boldsymbol{r}_{(j)}$. As one can see, equation (15) also contains the two-point PDF f_2 which is tantamount to the well-known *closure problem* in turbulence. In fact, the general n-point evolution equation in difference formulation, derived by Ulinich & Lyubimov (1968), is similar in structure and reads

$$
\begin{aligned}
&\frac{\partial f_n}{\partial t} + \boldsymbol{v}\cdot\nabla_{\boldsymbol{x}} f_n + \sum_{l=2}^{n}\Big[\boldsymbol{w}_{(l)}\cdot\nabla_{\boldsymbol{r}_{(l)}} f_n \\
&\quad +\nabla_{\boldsymbol{w}_{(l)}}\cdot\int \nabla_{\boldsymbol{r}_{(n+1)}}\big(G(\boldsymbol{r}_{(n+1)}-\boldsymbol{r}_{(l)})-G(\boldsymbol{r}_{(n+1)})\big) \\
&\quad\quad \times(\boldsymbol{w}_{(n+1)}\cdot\nabla_{\boldsymbol{r}_{(n+1)}})^2 f_{n+1}\,\mathrm{d}\boldsymbol{w}_{(n+1)}\mathrm{d}\boldsymbol{r}_{(n+1)} \\
&\quad +\nu\nabla_{\boldsymbol{w}_{(l)}}\cdot\int \big(\delta(\boldsymbol{r}_{(n+1)}-\boldsymbol{r}_{(l)})-\delta(\boldsymbol{r}_{(n+1)})\big) \\
&\quad\quad \times\boldsymbol{w}_{(n+1)}\Delta_{\boldsymbol{r}_{(n+1)}} f_{n+1}\,\mathrm{d}\boldsymbol{w}_{(n+1)}\mathrm{d}\boldsymbol{r}_{(n+1)}\Big] \\
&\quad +\nabla_{\boldsymbol{v}}\cdot\int \nabla_{\boldsymbol{r}_{(n+1)}} G(\boldsymbol{r}_{(n+1)}) \\
&\quad\quad \times(\boldsymbol{w}_{(n+1)}\cdot\nabla_{\boldsymbol{r}_{(n+1)}})^2 f_{n+1}\,\mathrm{d}\boldsymbol{w}_{(n+1)}\mathrm{d}\boldsymbol{r}_{(n+1)} \\
&\quad +\nu\nabla_{\boldsymbol{v}}\cdot\int \boldsymbol{w}_{(n+1)}\Delta_{\boldsymbol{r}_{(n+1)}} f_{n+1} \\
&\quad\quad \times\,\delta(\boldsymbol{r}_{(n+1)})\,\mathrm{d}\boldsymbol{w}_{(n+1)}\mathrm{d}\boldsymbol{r}_{(n+1)} = 0 \qquad (16)
\end{aligned}
$$

Again one observes that every n-point equation not only depends on f_n but also on the $(n+1)$-point PDF f_{n+1}.

Not surprisingly, the hierarchy (16) admits the same symmetries as the underlying Navier-Stokes equations, also referred to as classical symmetries, see (Wacławczyk *et al.*, 2014). In the same work, the authors also translated the statistical symmetries of the multi-point moment equations (5), given by a_{Ss} in (7) and by (8), to the LMN-hierarchy (16). In the variables of the PDF formulation the former (i.e. associated to a_{Ss} in (7)) is of the form

$$
\begin{aligned}
T_{Ss}:\quad & t^* = t,\quad \boldsymbol{x}^* = \boldsymbol{x},\quad \boldsymbol{r}^*_{(j)} = \boldsymbol{r}_{(j)},\quad \boldsymbol{v}^* = \boldsymbol{v},\quad \boldsymbol{w}^*_{(j)} = \boldsymbol{w}_{(j)}, \\
& f_n^* = \mathrm{e}^{a_{Ss}} f_n + (1-\mathrm{e}^{a_{Ss}})\delta(\boldsymbol{v})\delta(\boldsymbol{W}) \qquad (17)
\end{aligned}
$$

which was connected by Wacławczyk *et al.* (2014) to the phenomenon of intermittency. This can be best understood by noting that the delta distribution in (17) corresponds to the PDF of a laminar flow. The aforementioned symmetry thus combines laminar and turbulent components. The corresponding turbulent signal thus has an intermittent form. The second symmetry related to (8) has the form

$$
\begin{aligned}
T_{\mathrm{sh}}:\quad & t^* = t,\quad \boldsymbol{x}^* = \boldsymbol{x},\quad \boldsymbol{r}_k^* = \boldsymbol{r}_k,\quad \boldsymbol{v}^* = \boldsymbol{v},\quad \boldsymbol{w}^* = \boldsymbol{w}, \\
& f_n^* = f_n + \psi(\boldsymbol{v})\delta(\boldsymbol{W}) \qquad (18)
\end{aligned}
$$

describing non-Gaussian behaviour of turbulence. Here $\boldsymbol{W} = (\boldsymbol{w}_2,\dots,\boldsymbol{w}_n)$ and $\psi(\boldsymbol{v})$ has to admit the side condition $\int \psi(\boldsymbol{v})\,\mathrm{d}\boldsymbol{v} = 0$.

For the construction of invariant PDFs, in addition to the two statistical symmetries (17) and (18) above, also the classical symmetries of scaling in space $T_{\mathrm{sc},\boldsymbol{x}}$, scaling in time $T_{\mathrm{sc},t}$, and the three-parameter group spatial translations $T_{\mathrm{tr},\boldsymbol{x}}$ are considered. In the PDF formulation, the associated symmetry transformations have the form

$$
\begin{aligned}
T_{\mathrm{sc},\boldsymbol{x}}:\quad & t^* = t,\quad \boldsymbol{x}^* = \mathrm{e}^{a_{Sx}}\boldsymbol{x},\quad \boldsymbol{r}^*_{(k)} = \mathrm{e}^{a_{Sx}}\boldsymbol{r}_{(k)},\quad \boldsymbol{v}^* = \mathrm{e}^{a_{Sx}}\boldsymbol{v} \\
& \boldsymbol{w}^*_{(k)} = \mathrm{e}^{a_{Sx}}\boldsymbol{w}_{(k)},\quad f_n^* = \mathrm{e}^{-3na_{Sx}} f_n \qquad (19) \\
T_{\mathrm{sc},t}:\quad & t^* = \mathrm{e}^{a_{St}} t,\quad \boldsymbol{x}^* = \boldsymbol{x},\quad \boldsymbol{r}^*_{(k)} = \boldsymbol{r}_{(k)},\quad \boldsymbol{v}^* = \mathrm{e}^{-a_{St}}\boldsymbol{v} \\
& \boldsymbol{w}^*_{(k)} = \mathrm{e}^{-a_{St}}\boldsymbol{w}_{(k)}\quad,\quad f_n^* = \mathrm{e}^{3na_{St}} f_n \qquad (20) \\
T_{\mathrm{tr},\boldsymbol{x}}:\quad & t^* = t,\quad \boldsymbol{x}^* = \boldsymbol{x} + \boldsymbol{a}_{\boldsymbol{x}}\quad \boldsymbol{r}^*_{(k)} = \boldsymbol{r}_{(k)}\quad \boldsymbol{v}^* = \boldsymbol{v} \\
& \boldsymbol{w}^*_{(k)} = \boldsymbol{w}_{(k)},\quad f_n^* = f_n \qquad (21)
\end{aligned}
$$

where a_{Sx}, a_{St} denote two real parameters and $\boldsymbol{a}_{\boldsymbol{x}} = a_{\boldsymbol{x},1}$ denotes the three-dimensional parameter for the spatial translation group.

Using standard techniques of symmetry analysis, the condition for a hierarchy of PDFs $\{f_n : n = 1,2,3,\dots\}$ to be invariant w.r.t. to a one-parameter group T generated by a combination of T_{Ss}, T_{sh}, $T_{\mathrm{sc},\boldsymbol{x}}$, $T_{\mathrm{sc},t}$, $T_{\mathrm{tr},\boldsymbol{x}}$ for a given set of parameters a_{Ss}, ψ, a_{Sx}, a_{St}, $\boldsymbol{a}_{\boldsymbol{x}}$ is expressed by the condition to solve the following system of so-called *characteristic equations*

$$
\begin{aligned}
&\frac{\mathrm{d}t}{a_{St}t} = \frac{\mathrm{d}\boldsymbol{x}}{a_{Sx}\boldsymbol{x}+\boldsymbol{a}_{\boldsymbol{x}}} = \frac{\mathrm{d}\boldsymbol{r}_{(2)}}{a_{Sx}\boldsymbol{r}_{(2)}} = \dots = \frac{\mathrm{d}\boldsymbol{r}_{(n)}}{a_{Sx}\boldsymbol{r}_{(n)}} \\
&= \frac{\mathrm{d}\boldsymbol{v}}{(a_{Sx}-a_{St})\boldsymbol{v}} = \frac{\mathrm{d}\boldsymbol{w}_{(2)}}{(a_{Sx}-a_{St})\boldsymbol{w}_{(2)}} = \dots = \frac{\mathrm{d}\boldsymbol{w}_{(n)}}{(a_{Sx}-a_{St})\boldsymbol{w}_{(n)}} \\
&= \frac{\mathrm{d}f_n}{-\big[3n(a_{Sx}-a_{St})-a_{Ss}\big]f_n + \big[\psi(\boldsymbol{v})-a_{Ss}\delta(\boldsymbol{v})\big]\delta(\boldsymbol{W})} \qquad (22)
\end{aligned}
$$

This is a system of hyperbolic ordinary differential equations (ODEs) and can therefore be solved by the standard *method of characteristics*, see e.g. Cantwell (2002) for details and a general introduction to symmetry analysis.

Solving the system (22) for $n = 1$ and $a_{Sx} \neq 0$ as an ODE in the variable x_2 yields the following expression for an invariant one-point PDF

$$
\begin{aligned}
f_1(\boldsymbol{v};x_2) &= \tilde{x}_2^{\frac{-3(a_{Sx}-a_{St})+a_{Ss}}{a_{Sx}}}\,\tilde{f}_1\left(\tilde{x}_2^{\frac{a_{St}}{a_{Sx}}-1}\boldsymbol{v}\right) \\
&\quad + \frac{\tilde{x}_2^{\frac{-3(a_{Sx}-a_{St})+a_{Ss}}{a_{Sx}}}}{a_{Sx}-a_{St}}\int_1^{\tilde{x}_2^{1-\frac{a_{St}}{a_{Sx}}}} \tilde{s}^{2-\frac{a_{Ss}}{a_{Sx}-a_{St}}}\times \\
&\quad \times\psi\left(\tilde{s}\tilde{x}_2^{\frac{a_{St}}{a_{Sx}}-1}\boldsymbol{v}\right)\mathrm{d}\tilde{s} + f_1^{(\mathrm{i})}(\boldsymbol{v};x_2) \qquad (23)
\end{aligned}
$$

where $\tilde{x}_2 = Cx_2 + a$ for some constants $C > 0$ and a, $\tilde{f}_1(\boldsymbol{v})$ denotes a free PDF in one velocity variable and $f_1^{(\mathrm{i})}(\boldsymbol{v},\boldsymbol{x}) = \left(1-\tilde{x}_2^{a_{Ss}/a_{Sx}}\right)\delta(\boldsymbol{v})$ is the solution component due to the statistical scaling (17). This component, however, is usually not visible in data due to the delta function. Since the expressions in $\tilde{x}_2$ appearing in (23) have arbitrary real exponents, the expression (23) is only defined for $x_2 > -a/C$. Finally, similar expressions can be derived from (22) for the n-point PDFs f_n by the same methods. The resulting invariant expression is

$$f_n(\boldsymbol{v},\boldsymbol{W};x_2)=\tilde{x}_2^{-\frac{3n(a_{Sx}-a_{St})+a_{Ss}}{a_{Sx}}}\times$$
$$\times\tilde{f}_n\left(\tilde{x}_2^{\frac{a_{St}}{a_{Sx}}-1}\boldsymbol{v},\tilde{x}_2^{\frac{a_{St}}{a_{Sx}}-1}\boldsymbol{W}\right)+\Big(f_1^{(\mathrm{i})}(\boldsymbol{v};x_2)$$
$$+f_1^{(\mathrm{s})}(\boldsymbol{v};x_2)\Big)\delta(\boldsymbol{W})\qquad(24)$$

where the short-hand notation $f_1^{(\mathrm{s})}$ was used for the term in (23) with the integral over $\psi(\boldsymbol{v})$, i.e.

$$f_1^{(\mathrm{s})}(\boldsymbol{v},x_2)=\frac{\tilde{x}_2^{\frac{-3(a_{Sx}-a_{St})+a_{Ss}}{a_{Sx}}}}{a_{Sx}-a_{St}}\int_1^{\tilde{x}_2^{1-\frac{a_{St}}{a_{Sx}}}}\tilde{s}^{2-\frac{a_{Ss}}{a_{Sx}-a_{St}}}\times$$
$$\times\psi\left(\tilde{s}\tilde{x}_2^{\frac{a_{St}}{a_{Sx}}-1}\boldsymbol{v}\right)\mathrm{d}\tilde{s}\qquad(25)$$

and $f_1^{(\mathrm{i})}$ the same as in (23).

An important observation is that by using the PDF-based definition of the moments

$$\overline{U_1^n}=\int f_1(v_1;x_2)v_1^n\mathrm{d}v_1\qquad(26)$$

for the invariant PDF (23), the resulting moment expressions are in complete agreement with the invariant moment scaling laws (9)-(10) and (12), using the corresponding scaling parameters κ, ω, σ_1 and σ_2. Three cases may be distinguished. More precisely, taking $n(a_{Sx}-a_{St})+a_{Ss}=0$, for a fixed n the expression derived from (23) via (26) for this n-th moment are given by a log-function

$$\overline{U_1^n}(x_2)=\tilde{H}_n+\frac{A_n}{a_{Sx}}\ln(\tilde{x}_2)\qquad(27)$$

where the constants $\tilde{H}_n, A_n$ are defined as

$$\tilde{H}_n=\int\tilde{v}_1^n\tilde{f}_1(\tilde{\boldsymbol{v}})\,\mathrm{d}\tilde{\boldsymbol{v}}\quad,\quad A_n=\int\tilde{v}_1^n\psi(\tilde{\boldsymbol{v}})\,\mathrm{d}\tilde{\boldsymbol{v}}\qquad(28)$$

All other moments then turn out to be power laws. Physically relevant seem to be the following cases.

For the classical log-law, i.e. for $a_{Sx}-a_{St}+a_{Ss}=0$, one obtains (9) from (27) by setting $A_1=u_\tau a_{Sx}/\kappa$, $\tilde{H}_1=u_\tau B$ and $C=1/(\nu\sqrt{\rho/\tau_w})$, $a=0$ in the notation $\tilde{x}_2=Cx_2+a$ introduced above, since then $\tilde{x}_2=y^+$ is the distance to the wall in wall units. Similarly, for $n\geq 2$ the scaling law of higher moments (10) follows from (29) below by setting $A_n=(n-1)a_{Sx}\omega u_\tau^n B_n$ and $\tilde{H}_n=u_\tau^n(C_n-B_n)$. In fact, recalling that $\omega=(a_{Sx}-a_{St})/a_{Sx}$, this choice reduces (30) to $\tilde{D}_n=-u_\tau^n B_n$ and hence $D_n=\tilde{H}_n-\tilde{D}_n=u_\tau^n C_n$.

In the case of the deficit power-law, i.e. $n(a_{Sx}-a_{St})+a_{Ss}\neq 0$, the corresponding result for the n-th moment are

$$\overline{U_1^n}(x_2)=\tilde{x}_2^{\frac{n(a_{Sx}-a_{St})+a_{Ss}}{a_{Sx}}}D_n+\tilde{D}_n\qquad(29)$$

where $D_n=\tilde{H}_n-\tilde{D}_n$ and $\tilde{D}_n$ is short-hand notation for

$$\tilde{D}_n=\frac{-A_n}{n(a_{Sx}-a_{St})+a_{Ss}}\qquad(30)$$

Now the deficit law (12) can be obtained from (29) by setting $A_n=-(n(a_{Sx}-a_{St})+a_{Ss})\overline{U_1^n}^{(0)}$ and $\tilde{H}_n=\overline{U_1^n}^{(0)}-u_\tau^n C_n'$ while setting $C=1/h$ and $a=0$ in the definition of $\tilde{x}_2$. Indeed, the choice for A_n yields $\tilde{D}_n=\overline{U_1^n}^{(0)}$ in (30) and $D_n=-u_\tau^n C_n'$.

In view of definition (28) the constants A_n are essentially the moments of the distribution function $\psi(\boldsymbol{v})$. By definition (30) of the $\tilde{D}_n$, the relation $\tilde{D}_n=\overline{U_1^n}^{(0)}$ used above to obtain the deficit law (12) from (29) implies that the moments of the function $\psi(\boldsymbol{v})$ are determined by the moments $\overline{U_1^n}^{(0)}$ of the PDF $f_1^{(0)}(\boldsymbol{v})=f_1(\boldsymbol{v};0)$ at the centre of the channel. Assuming that all moments $\overline{U_1^n}^{(0)}$ exist and the corresponding moment problem can be solved positively for the A_n, this means that the function $\psi(\boldsymbol{v})$ can be expressed in terms of the PDF $f_1^{(0)}(\boldsymbol{v})$. That suggests the possibility of formulating a deficit law for PDFs similar to (12).

The question whether not only the derived moment expressions (9), (10) and (12) are in good agreement with the DNS data but also the proposed invariant PDF scaling law (23) is an open question and subject of current research.

CONCLUSIONS AND OUTLOOK

The central result of the present contribution is that, on the basis of classical and statistical symmetries, we are now able to calculate invariant solutions for moments of arbitrary order as well as for the corresponding PDF for near-wall shear flows. It is particularly important that the moments and the PDFs are based on the instantaneous velocities and not on the fluctuation velocities resulting from the Reynolds decomposition.

The final step is the determination of the free function ψ, which characterises non-Gaussian behaviour in (18), which explicitly appears in the PDF solution (23), and needs to be determined from DNS data.

REFERENCES

Avsarkisov, V., Oberlack, M. & Hoyas, S. 2014 New scaling laws for turbulent poiseuille flow with wall transpiration. *Journal of Fluid Mechanics* **746**, 99–122.

Barenblatt, G. I. 1993 Scaling laws for fully developed turbulent shear flows. part 1. basic hypotheses and analysis. *Journal of Fluid Mechanics* **248**, 513–520.

Cantwell, Brian J. 2002 *Introduction to Symmetry Analysis*, 1st edn., *Cambridge Texts in Applied Mathematics*, vol. 29. Cambridge University Press.

von Kármán, T. 1930 Mechanische Ähnlichkeit und Turbulenz. *Nachr. Ges. Wiss. Göttingen* **58-76**.

von Kármán, Theodore & Howarth, Leslie 1938 On the statistical theory of isotropic turbulence. *Proceedings of the Royal Society of London. Series A-Mathematical and Physical Sciences* **164** (917), 192–215.

Lee, M.K. & Moser, R.D. 2015 Direct numerical simulation of turbulent channel flow up to $Re_\tau \approx 5200$. *Journal of Fluid Mechanics* **774**, 395–415.

Lundgren, L. 1967 Distribution functions in the statistical theory of turbulence. *Physics of Fluids* **10(5)**, 969–975.

Monin, A. S. 1967 Equations of turbulent motion: PMM vol. 31, no. 6, 1967, pp. 1057–1068. *Journal of Applied Mathematics and Mechanics* **31** (6), 1057–1068.

Oberlack, Martin 2001 A unified approach for symmetries in plane parallel turbulent shear flows. *Journal of Fluid Mechanics* **427**, 299–328.

Oberlack, M., Hoyas, S., Kraheberger, St., Alcántara-Ávila, F. & Laux, J. 2022 Turbulence Statistics of Arbitrary Moments of Wall-Bounded Shear Flows: A Symmetry Approach. *Phys. Rev. Lett.* **128** (2), 024502, publisher: American Physical Society.

Oberlack, M. & Rosteck, A. 2010 New statistical symmetries of the multi-point equations and its importance for turbulent scaling laws. *Discrete Continuous Dyn. Syst* **3**, 451–471.

Oberlack, Martin, Wacławczyk, Marta, Rosteck, Andreas & Avsarkisov, Victor 2015 Symmetries and their importance for statistical turbulence theory. *Mechanical Engineering Reviews* **2** (2), 15–00157.

Sadeghi, H., Oberlack, M. & Gauding, M. 2018 On new scaling laws in a temporally evolving turbulent plane jet using lie symmetry analysis and direct numerical simulation. *Journal of Fluid Mechanics* **854**, 233–260.

Ulinich, F. & Lyubimov, B. 1968 The statistical theory of turbulence in an incompressible fluid at high Reynolds numbers. *Journal of Experimental and Theoretical Physics* **55**, 44.

Wacławczyk, M., Staffolani, N., Oberlack, M., Rosteck, A., Wilczek, M. & Friedrich, R. 2014 Statistical symmetries of the lundgren-monin-novikov hierarchy. *Physical Review E* **90** (1), 013022.